Revista de Climatología

Vol. 9 (2009): 45-61 ISSN 1578-8768

Observed changes in extreme temperatures over Spain during 1957-2002, using Weather Types

M. Bermejo[1] and R. Ancell[2]

AEMET, Delegación Territorial en Cantabria ([1]mbermejo@inm.es, [2]rct@inm.es)

(Recibido: 01-Sep-2009. Publicado: 22-Dic-2009)

Abstract

The aim of this paper is to identify and analyze the daily variability of observed changes in the extreme temperatures in relation to the atmospheric circulation. In order to carry this out, a joint probabilistic analysis of Weather Types (WTs) and the corresponding surface observations has been performed, comparing daily surface observations of extreme temperatures, in two different periods of time (1957-1979 and 1980-2002) over mainland Spain and the Balearic Islands. The results show that there were significant changes in the extreme temperatures between the two periods of study; moreover, these changes were heterogeneous in space, time and WT. Finally, we have noticed that these observed alterations were more related to changes in the extreme temperatures of the corresponding WTs than to changes in the occurrence probability of the WTs.

Key words: Weather Types, extreme temperatures, daily data, observed climate change.

Resumen

El objetivo principal de este artículo es identificar y analizar la variabilidad a escala diaria de los cambios observados en las temperaturas extremas en relación a la circulación atmosférica, realizando un análisis probabilístico conjunto de Tipos de Tiempo y sus correspondientes observaciones meterológicas en superficie. Para ello, en este estudio hemos comparado observaciones diarias de temperaturas extremas en superficie, en dos periodos de tiempo (1957-1979 y 1980-2002) en la España continental y las islas Baleares. Los resultados muestran diferencias significativas entre los dos periodos de estudio; además, estos cambios en las temperaturas extremas fueron heterogéneos en espacio, tiempo y Tipo de Tiempo. Por último, hemos comprobado que las alteraciones observadas están más relacionadas con cambios en las temperaturas extremas de los Tipos de Tiempo correspondientes que con cambios en la probabilidad de ocurrencia de los mismos.

Palabras clave: *Tipos de Tiempo, temperaturas extremas, dato diario, cambio climático observado.*

1. Introduction

Atmospheric variability and changes in surface observations have a strong cause-effect relationship; for instance, variations in the composition of the atmosphere, cause an impact over the variability of the climatic system at all scales (Lamb, 1977; Diaz, 1981). Therefore, observed alterations in the climate can be considered as an effect of changes in the atmospheric variability, particularly at daily timescale. From this point of view, the aim of this work consists in analyzing the relationship between alterations in the atmospheric variability and changes in meteorological surface observations at daily timescale, in two recent periods: 1957-1979 and 1980-2002. We hope that this will allow us to better understand the complex inter-relationship between some climatic forcings and their possible local scale impacts.

Although weather situations are never exactly repeated, many common features can be found in a series of synoptic weather maps over a long period of time. Weather Types (WTs), or *Circulation Classifications* (as defined by the European Cooperation in Science and Technology, Action COST 733 (2005)) are generalized synoptic situations obtained from classifying typical atmospheric patterns over a specified domain (Lamb, 1972) and they are widely used in meteorological applications and climate research.

Therefore, in order to analyze the atmospheric behavior, we have used the concept of WTs.

There are some previous works that used a WT classification to study the influence of the atmospheric circulation on surface observations. Recently, Jones and Lister (2009) have studied seasonal changes between three different periods of time, in daily temperature, precipitation and Diurnal Temperature Range (DTR) across Europe, with the aim of finding wether these changes where related to long-term warming over the domain or associated with warming within some of the WTs. There are some other works also focused over the European domain: Bárdossy and Caspary (1990) and Esteban *et al.* (2006). In the former, the authors studied the observed changes in the annual and monthly frequency of different patterns over Europe. In the latter, the authors used the NCEP/NCAR Reanalysis Project data, in order to create a daily catalogue of the circulation patterns over the domain, but they did not study changes in the corresponding surface observations related to these patterns. Considering a smaller domain, Brunet *et al.* (2007) analyzed spatial patterns of temperature change over Spain during period 1850-2005, using daily maximum, minimum and mean temperatures from 22 stations, considered to be the longest and the most reliable ones over the domain.

In our work we will show the changes found in surface observations, during 1957-2002 over Spain, for maximum and minimum temperatures. We will also show the changes found on the WTs and we will try to explain the relationship between these two changes.

The organization of the paper is as follows: the domain of study, the daily data series and the atmospheric data will be presented in section 2. Section 3 will describe the time series homogenization process and it will also give a brief description of the WTs classification. The results will be exposed in section 4 and section 5 will show the discussions and conclusions of this work.

2. Data

This study has been carried out for mainland Spain and the Balearic Islands domain (see figure 1), using Re-analysis data from Atmospheric Circulation Models (ACMs) and surface historic observation records.

We have divided the time series, that will be described below, into two periods, which are similar in length: 1957-1979 and 1980-2002.

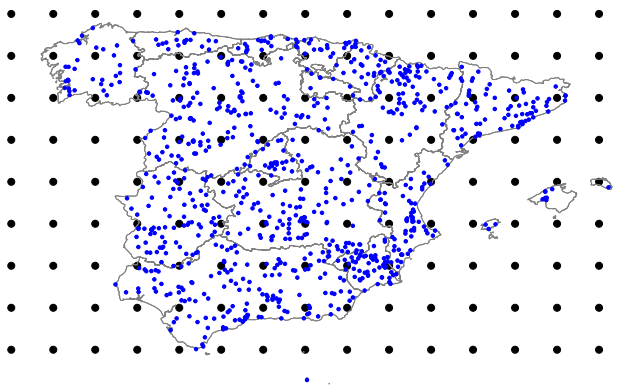

Figure 1: The black thick dots represent ERA-40 1° resolution grid points and the smaller blue dots show the location of the 888 thermometric stations selected for this study.

2.1. Atmospheric Data

To an operative level, ACMs are numerically integrated discretizing space and time (from an initial condition), in order to periodically estimate the values of atmospheric variables in determined points of a 3D-grid, like that associated to our domain (see figure 1). In this case, the Re-analysis data of ERA-40 (Uppala *et al.*, 2005), from the model of the European Meteorology Center (ECMWF), have been used.

This provides data of the atmospheric state every 6 hours, for the period starting on September 1^{st} of 1957 and ending on August 30^{th} of 2002, with a 1° horizontal resolution, approximately. Table 1 shows the variables we have used.

Table 1: ERA-40 Re-analysis fields used to classify the WTs

Variables		Levels (hPa)	UTC hours
T	Temperature	1000	00
Z	Geopotencial Height	850	06
R	Relative Humidity	700	12
U	E Wind Component		18
V	N Wind Component		

2.2. Observations Data

The other data set we have used, is the Spanish Meteorological Agency's (AEMET, *Agencia Estatal de Meteorología*) observations network, which gives us an idea of the meteorological phenomena on surface, over the domain of study. Daily maximum and minimum temperature data have been used, for the same time period as the ERA-40 Re-analysis data. There are 3109 thermometric stations available, from the AEMET's network, divided into the 11 basins of our domain (see the right figure in figure 3). To make sure that our statistical model will be able to correctly fit the parameters, we have eliminated those time series with scarce data, considering only those series with, at least, 15% of the data in each of the two periods mentioned above. This leaves us 1061 stations, at this stage.

3. Methodology

3.1. Data homogenization

Although data have been filtered, we need to make sure that the variability of the time series is mainly a response of the atmospheric variability, so inhomogeneous stations at daily timescale must be excluded. In order to perform this, we have used as absolute homogeneity criterion (Conrad and Pollack, 1962) the predictive capability, in terms of Root Mean Squared Error (RMSE), of the standard analogues method (Lorenz, 1969) using the ERA-40 Re-analysis data. We do not use the Alexandersson's test (Alexandersson, 1986) because we are considering extreme temperature data, which are not independent and are not identically distributed at daily resolution (Cano and Gutiérrez, 2004). To validate this procedure, we have randomly selected 10% of the data of each series as the test sample and the left data in each series will be treated as the train sample.

Figure 2 shows the results for maximum and minimum temperatures. In this figure, stations have been divided into groups of ten percentiles according to the values of RMSE in each basin. This is, the first box plot in each figure (2(a) for maximum temperature and 2(b) for minimum temperature) represents the RMSE of a group of stations made up by the 10% of the stations with the highest RMSE in each basin and so on. We can see that the RMSE of the first 10% of the stations is clearly higher than the RMSE of the rest of the groups of stations, for both maximum and minimum temperatures. This provides us a reasonable criterion to eliminate them, because it means that an important part of the variability of these stations is badly related to the atmosphere. After this, we ended up with 888 stations, and their distribution over the domain is shown in figure 1. As we can see, the stations are quite well spread, covering the whole area without leaving any region sparse. The left table in figure 3 shows how many stations are left in each basin after every filtering stage.

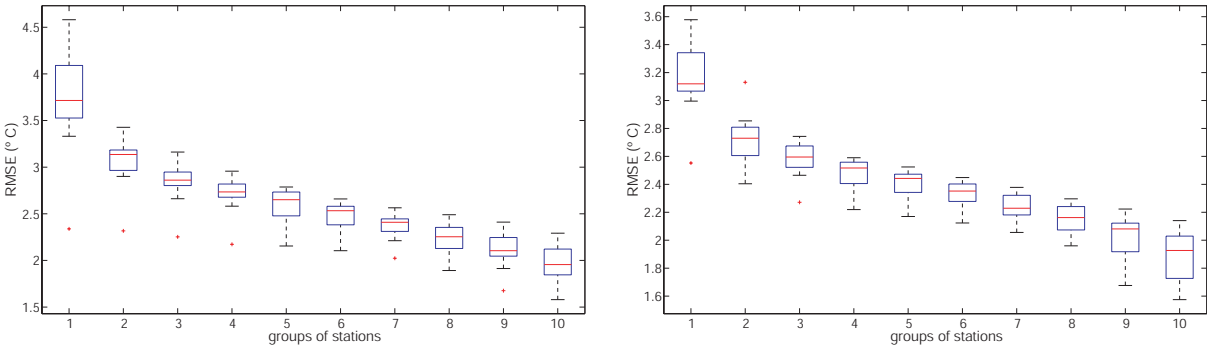

(a) Maximum Temperature (b) Minimum Temperature

Figure 2: Box plot of the Root Mean Squared Error for maximum temperature 2(a) and minimum temperature 2(b), in °C, for the 1061 stations of the domain. We have made groups of 10% of stations, according to the value of the RMSE in each basin.

Basins	**Initial Stations**	**At least 15% data**	**Final Stations**
North	436	110	94
Duero	315	152	126
Tajo	261	95	81
Guadiana	369	145	121
Guadaquivir	318	92	78
South	137	57	48
Segura	220	101	83
Levante	338	84	69
Ebro	417	153	128
Cataluña	236	59	49
Baleraric	62	13	11
Total Domain	3109	1061	**888**

Figure 3: On the *left table*; **Initial Stations**: number of stations in each basin available from the AEMET's Network; **At least 15% data**: number of stations with at least 15% data in both periods of study (1957-1979 and 1980-2002); **Final stations**: number of stations after eliminating the worst 10% of the stations, in terms of RMSE, in each basin. These are the stations shown in figure 1 and the ones used in this work. The *right figure* shows the 11 basins into which our domain is divided: North, Duero, Tajo, Guadiana, Guadalquivir, South, Segura, Levante, Ebro, Cataluña and Balearic. Notice that the Balearic Islands basin is not shown in this figure, but it will be included in the study.

Now that we have made sure that the whole area is well represented by these 888 stations, we need to remove suspicious data. We have considered those values that are repeated five or more consecutive days as missing data, because this indicates that there has probably been a mistake measuring the variables during those days. The percentage of missing data in each basin, including those introduced by eliminating these suspicious data, is shown in table 2.

The homogenization process has been carried out in two steps:

In the first step, broadening the field of action of the absolute homogeneity criterion, we have considered the first 50 Principal Components (PCs) of the ERA-40 selected variables (which explain the 95% of the total variance) as predictors, to reconstruct the observed series by means of a statistical downscaling method based on a linear multiple regression model:

$$\hat{Y} = \theta_{abs} \cdot PC \tag{1}$$

Table 2: **RMSE** values correspond to the median of RMSE for the **test** and **train** sample of each basin for maximum (**Tx**) and minimum (**Tn**) temperatures. **Outliers (%)**: percentage of outliers in each basin for **Tx** and **Tn** (outliers in the second step of the homogenization); **Missing (%)**: percentage of total missing values in each basin.

Basins	**RMSE (test)**		**RMSE (train)**		**Outliers (%)**		**Missing (%)**	
	Tx	**Tn**	**Tx**	**Tn**	**Tx**	**Tn**	**Tx**	**Tn**
North	1.886	1.646	1.738	1.521	0.052	0.069	32.694	32.822
Duero	1.865	1.673	1.774	1.560	0.010	0.042	26.370	26.477
Tajo	1.954	1.795	1.849	1.666	0.007	0.027	33.407	33.542
Guadiana	1.871	1.685	1.795	1.574	0.009	0.037	33.369	33.547
Guadaquivir	1.969	1.795	1.867	1.677	0.020	0.061	38.737	39.783
South	2.142	1.932	2.063	1.781	0.068	0.093	38.441	38.810
Segura	1.889	1.705	1.857	1.601	0.019	0.041	22.290	22.589
Levante	1.576	1.589	1.459	1.444	0.014	0.021	30.593	30.687
Ebro	1.798	1.600	1.685	1.518	0.012	0.031	34.163	34.338
Cataluña	1.543	1.496	1.412	1.364	0.026	0.023	41.052	41.121
Baleraric	1.495	1.495	1.359	1.430	0.011	0.018	40.713	40.696

Equation 1 is a matrix equation, where θ_{abs} is the regression matrix, *PC* is the predictors matrix, and $\hat{Y}$ is the first guess reconstructed data matrix.

The second step of the homogenization process is a relative homogenization. Here, we have used the information given by the neighboring stations to reconstruct the series, but this time, instead of the atmospheric PCs, we have used data from the rest of the stations in the same basin as predictors:

$$\hat{Z} = \theta_{rel} \cdot \hat{Y} \tag{2}$$

Equation 2 is another matrix equation. θ_{rel} is the regression matrix of the relative homogenization, $\hat{Y}$ is the resultant matrix of the estimated data in the first step of the homogenization and $\hat{Z}$ represents the final homogenized data set.

Combining equations 1 and 2 we will obtain

$$\hat{Z} = \theta_{rel} \cdot \theta_{abs} \cdot PC \tag{3}$$

In the relative homogenization step, outliers have been removed from the series. We have defined these outliers as those values whose error (the difference between the original series and the estimated ones) is outside the interval $\pm 1.645\sigma$ (which corresponds to a 90% of confidence level), where σ is the standard deviation of the original series.

Although all this process might seem quite simple, the resultant homogenized time series are reliable enough, because the median of the RMSE, for each basin, are not greater than 2°C (except for maximum temperature of the South basin), as we can see in table 2. This table shows the median of the test and train RMSE for maximum and minimum temperatures of each basin. The last four columns of this table show the percentage of outliers and of total missing values in each basin for each of the extreme temperatures.

The mean values of the Bias, for the test sample, for maximum and minimum temperatures are -0.011°C and -0.017°C, respectively. These values can be considered negligible, since they are one order of magnitude smaller than the observed trends, as it is shown in figure 4.

From now on, we will work with these homogenized series.

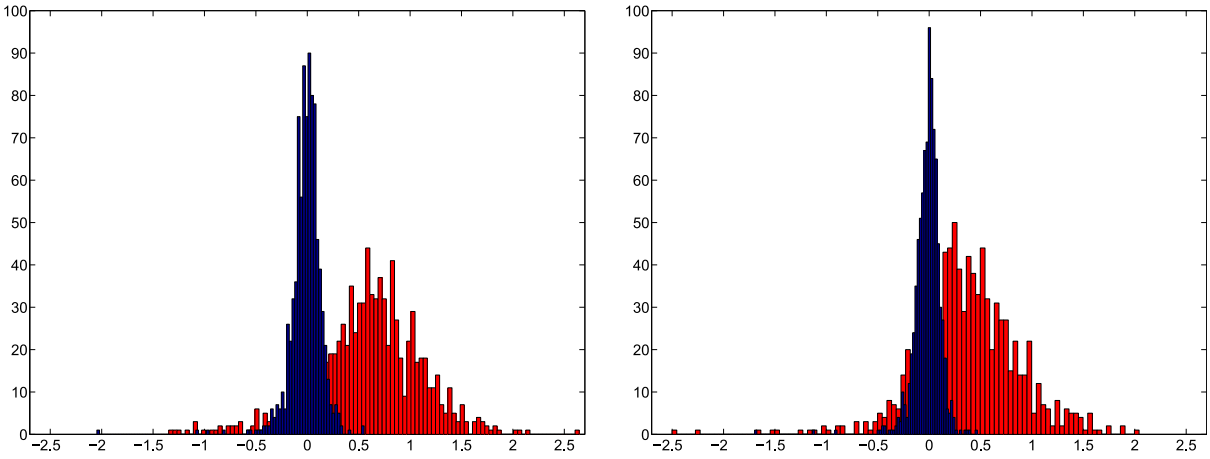

(a) Maximum Temperature (b) Minimum Temperature

Figure 4: In blue, histograms of the Bias of the test sample (°C). In red, histograms of the differences in temperature (°C), that will be shown in section 4. Figure 4(a) for maximum temperature and figure 4(b) for minimum temperature.

3.2. Circulation classification: Weather Types

Although this is not the first time that this kind of study has been performed, for a large-scale resolution in western Europe domain (Jones and Lister, 2009; Pastor *et al.*, 2008; Esteban *et al.*, 2006; Huth *et al.*, 1993; Bárdossy and Caspary, 1990), in this work we pretend to offer a local perspective of the problem, focusing in mainland Spain and the Balearic Islands domain.

To obtain WTs at daily timescale, we need to use algorithms able to distinguish meteorological situations, defined by circulation parameters. In order to do so, we have performed an objective classification of the atmospheric states, defined by the group of standard fields and levels given by ERA-40 in the domain shown in figure 1. The resultant daily patterns are of a very high dimension, because they are made up of 60 variables (5 atmospheric variables in 3 levels at 4 different time steps, see table 1) on each of the 15x9 nodes that delimitate our domain. Therefore, to manage them in an efficient and realistic way, we have used PCs techniques (Preisendorfer and Mobley, 1988), reducing their dimension to 50 in order to conserve 95% of the variance inside the domain. Once this is done, there are different strategies of classifying the atmospheric states: Neural Networks (Gutiérrez *et al.*, 2004b), simulated annealing clustering (Philipp *et al.*, 2007) or Bayesian Networks (Ancell and Gutiérrez, 2008), for instance. Among them, we have selected one of the most popular and simplest method, which is the *k-means* clustering algorithm (Anderberg, 1973), with the aim of globally minimizing the intra-classes distance, so as to classify the atmospheric states using k classes. The center of each one of these classes represents the group of atmospheric states considered to be the most related ones, according to the metric used in the algorithm, and, although it is not real, it can be considered as a Weather Type (WT). This way, the atmospheric state variable may be synthesized into a discrete scalar, which will allow us, not only to efficiently analyze changes in its probability distribution, but also to study changes in the intensity of the different phenomena associated to each WT.

It is particularly interesting, for meteorological and climatological purposes, the possibility of ordering WTs. In this case, the classification can be performed using a *Self-Organizing-Map* (SOM) clustering (Hewitson and Crane, 2002; Kohonen, 1997), which is an extension of the *k-means* clustering, and where the centers are forced to organize themselves by a second criterion of analogy.

In order to show the variability of the atmospheric state at daily timescale in a better way, it is interesting to have as many different WTs as possible. Thus, the greater the number of classes, the better each real atmospheric state will be represented by its corresponding WT. However, it is also necessary for each

class to have enough members, so that a robust statistical analysis can be performed, and this requires a smaller number of classes. Considering the length of the available time series and the spatio-temporal scale of the domain, different values of k have been tested and the best result, taking all the above requirements into account, has been obtained for *k=100*, with an average of 150 members per class (Gutiérrez *et al.*, 2004a).

Figure 5 shows the resulting *k-means* cluster used in this work, projected in the space of the first two PCs. In figure 5(a) the little grey dots represent each one of the atmospheric states, which are divided into classes, represented by cells in this figure. Black thick dots represent the centers of each class and these will be considered as the WTs. Figure 5(b) shows an enlargement of a particular class of the cluster, in which the blue little dots are the members of the class that happened during the first period (1957-1979), while the red crosses are those that appeared during the second period (1980-2002). The big blue circle represents the centroid for the atmospheric states of the first period and the big red circle is the centroid for those of the second period. This two new centroids will be considered as the WTs in each one of the periods mentioned, so we will have a cluster for each period, based on our general cluster (the centroid for the full series is represented by the grey big circle). This way we will be able to compare the WTs of both periods, in order to find changes in the behavior of the atmosphere.

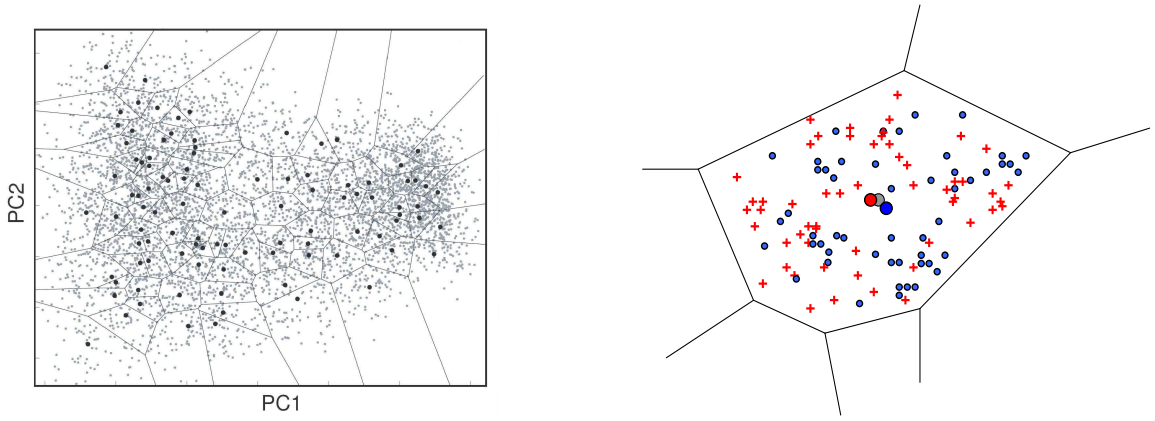

(a) cluster (b) a class of the cluster

Figure 5: Classification of the atmospheric states in 100 Weather Types by means of a *k-means* cluster. PC1 and PC2 are the first and second PCs, respectively. Figure 5(b) shows one of the classes of the cluster.

Once we have identified the WTs, they are very useful to obtain additional information. This information can be basically classified in three groups, depending on its relationship with:

- The occurrence probability of each WT; which is directly associated with the number of real atmospheric states that define it.
- The statistics (percentiles, means, extremes, etc) of the atmospheric variables and also of the meteorological observations, that can be obtained from each WT.
- The transition probability from one WT to another (this has not been considered in this work).

From all these aspects, we have focused our attention, not only on changes in WT's occurrence probability, but also on changes in the intensity of the associated phenomenology for each WT. The results will be shown in section 4.

4. Results

4.1. Spatial distribution

First of all, we will present some results about the character and magnitude of the spatial distribution of the observed changes. These results have been obtained using the homogenized data set, comparing extreme temperature surface observations during the two periods of study.

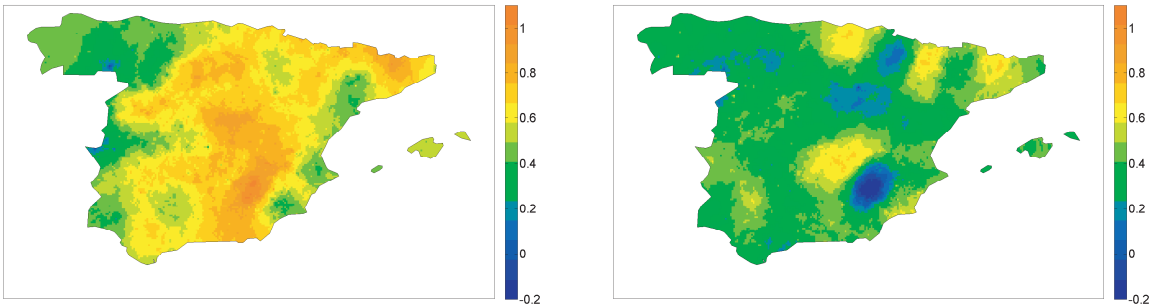

(a) Maximum Temperature (b) Minimum Temperature

Figure 6: Spatial distribution of absolute changes in extreme temperatures (°C) in period 1980-2002 with respect to 1957-1979 (figure 6(a) for maximum temperature and figure 6(b) for minimum temperature).

We have performed a Mann-Kendall test (Sneyers, 1975) of the null hypothesis of trend absence in the series, against the alternative of trend for a significance level of $\alpha = 0.05$, getting p-values close to zero in almost every location and, therefore, rejecting the null hypothesis. In figure 6 absolute changes in the behavior of the extreme temperatures are shown, relative to the first period (1957-1979). This means that positive/negative differences indicate that the magnitude has increased/decreased in the second period (1980-2002).

In accordance with the Mann-Kendall test results, a generalized rise in maximum and minimum temperature, since 1980, was observed. Moreover, we can conclude that maximum temperature rose more than minimum temperature for most of the regions.

For maximum temperature (figure 6(a)), the highest increase values were located over the Cataluña basin and the central strip of the peninsula, while the lowest increases were localized over western Spain.

For minimum temperature (figure 6(b)), the highest values were located over the Cataluña basin, the eastern side of the Guadiana basin and the eastern side of the North basin combined with the northwestern Ebro basin; and the lowest ones were found on the northwestern part of Spain, the south of the Ebro basin and the western side of the Segura basin (see the right figure in figure 3, to visualize the mentioned regions).

4.2. Temporal distribution

The same process has been carried out seasonally. In order to do so, we have considered December, January and February as the winter months; March, April and May as spring; June, July and August as summer; and September, October and November as the fall season. Figures 7 and 8 show the results for maximum and minimum temperatures, respectively. Notice that the scale is not always positive. This means that, for some seasons, there are areas that were cooler during the second period (1980-2002) than during the first one (1957-1979), hence, temperature dropped.

If we focus on maximum temperature, during winter time (figure 7(a)), the differences were positive over the whole domain, so, we can say that maximum temperature in winter became warmer during the second period, with the lowest values over the Mediterranean watershed (except the Cataluña basin)

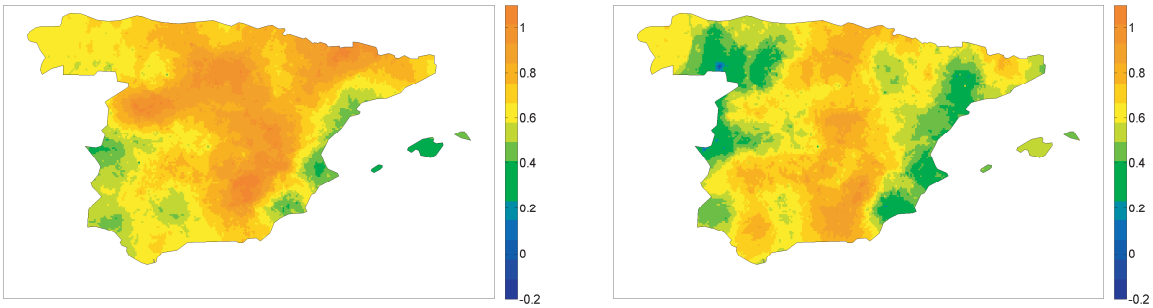

(a) DJF (b) MAM

(c) JJA (d) SON

Figure 7: Absolute changes in maximum temperature for each season (°C). Positive/negative changes indicate an increase/decrease in temperature for the second period of study (1980-2002). Notice that the scale is the same for the four seasons.

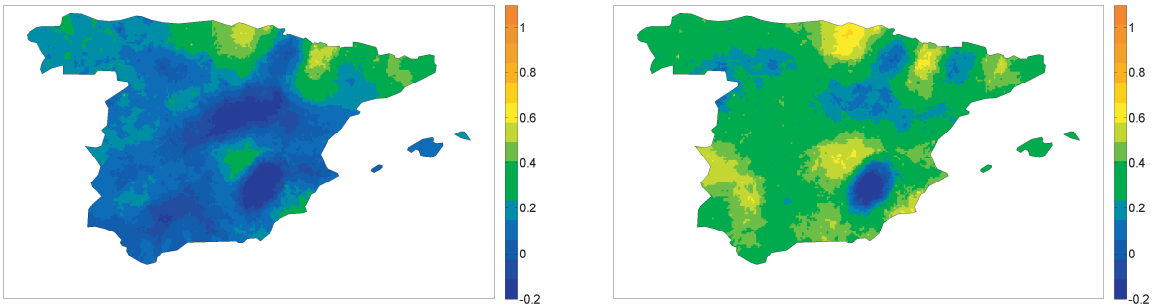

(a) DJF (b) MAM

(c) JJA (d) SON

Figure 8: The same as figure 7 but for minimum temperature (°C).

and the western side of the Guadalquivir and the Guadiana basins. In spring (figure 7(b)), temperature increased over almost all areas, being the Cataluña basin and the central strip of Spain the zones where maximum temperature rose more. Summer (figure 7(c)) divided the peninsula into two zones: maximum temperature hardly rose, or even decreased, over the western area, since 1980, while the middle and eastern areas were warmer during 1980-2002. Finally, during the fall season (figure 7(d)), changes were smaller. The Cataluña, the South and the Segura basins and also the eastern side of the North basin were the regions with higher rises in maximum temperature.

In the case of minimum temperature, we can see that it hardly changed or decreased in almost all areas during winter (figure 8(a)), with the exception of the northeastern area. Figure 8(b), spring, is similar in shape to figure 8(a), but with higher values. Summer (figure 8(c)) and, particularly, fall (figure 8(d)), showed the highest changes, which appeared over the Cataluña and the Guadalquivir basins, the western side of the Guadiana basin and the eastern side of the North basin. During these seasons there were little areas with negative changes in minimum temperature.

Table 3 shows these same results numerically, in °C/decade. The three tables represent the annual and seasonal changes in maximum (top table), minimum (middle table) and DTR (bottom table) for each basin. Some details, that we want to be noticed, have been remarked in bold: maximum temperature registered the highest increase during winter and minimum temperature showed the highest increase during autumn. This implies a higher DTR during winter, since 1980, and a lower DTR during fall.

It is now clear, from table 3 and figures 7 and 8, that the DTR during winter was higher for period 1980-2002 than for period 1957-1979. This is a local result that does not agree with the fourth IPCC global assessment (IPCC, 2007). Moreover, changes in maximum and minimum temperatures were different in magnitude and seasonal distribution. Maximum temperature changes were higher during winter, while minimum temperature changes were bigger during summer and autumn.

4.3. Circulation distribution

In this section, we have associated changes in the extreme temperatures distributions with changes in the atmospheric circulation, always the second period (1980-2002) minus the first period (1957-1979), performing a simple joint probabilistic analysis of the extreme temperatures, conditioned to WTs, from a collective behavior point of view.

In figure 9, the upper/middle panels represent the observed alterations in maximum/minimum temperatures, conditioned to each WT, and the bottom panel shows changes in the WTs' occurrence probability. The x-axis of the three panels represent the 100 WTs, ordered by their mean temperature (considered as the average of the extreme temperatures) during period 1957-1979. This way, the coolest WTs are located on the left side of the panels and the warmest ones on the right side.

First of all, we have made an analysis taking into account the maximum and minimum temperatures of each WT. This can be seen in the upper and middle panels of figure 9, respectively. 53% of the WTs rose their maximum temperature, while 30% of them decreased it, and 69% of the WTs rose their minimum temperature, whereas 17% of them dropped it (see table 4). This implies that most of the WTs became warmer from 1980 on, for both maximum and minimum temperature, and we can say that WTs increased their minimum temperature in a more generalized way than maximum temperature.

Furthermore, WTs with the highest mean temperature tend to rise their extreme temperatures, while WTs with the lowest mean temperature tend to decrease or maintain their extreme temperatures. Thus, WTs were getting more extreme, because high temperatures were even higher and low temperatures were even lower during the second period.

The results obtained for the occurrence probability of the WTs (bottom panel of figure 9) showed that the differences in the frequency of appearance of the WT, in some cases, are of the same order of magnitude than their own frequency of appearance, that is, ± 0.01 on average for 100 classes.

Table 3: Annual and seasonal trends in maximum temperature (top table), minimum temperature (middle table) and DTR (bottom table), for each basin and the total domain (°C/decade).

Δ Tx (°C/decade)	Annual	DJF	MAM	JJA	SON
North	0.24	0.32	0.31	0.14	0.16
Duero	0.25	**0.37**	0.20	0.21	0.09
Tajo	0.23	0.29	0.24	0.18	0.11
Guadiana	0.29	0.31	0.32	0.22	0.20
Guadaquivir	0.29	0.30	0.34	0.20	0.21
South	0.30	0.30	0.30	0.22	**0.33**
Segura	0.30	0.31	0.25	0.25	0.30
Levante	0.27	0.29	0.22	0.25	0.24
Ebro	0.29	0.37	0.26	0.25	0.17
Cataluña	**0.31**	0.29	0.26	**0.35**	0.28
Baleraric	0.21	0.07	0.27	0.28	0.20
Total Domain	0.27	**0.32**	0.27	0.22	0.19

Δ Tn (°C/decade)	Annual	DJF	MAM	JJA	SON
North	0.19	**0.14**	0.20	0.20	0.21
Duero	0.14	0.07	0.12	0.14	0.19
Tajo	0.15	-0.02	0.13	0.21	0.20
Guadiana	0.21	0.05	0.20	0.24	0.30
Guadaquivir	0.20	0	0.18	0.24	**0.31**
South	0.14	0.05	0.16	0.11	0.21
Segura	0.11	0	0.08	0.11	0.23
Levante	0.19	**-0.03**	0.17	0.23	0.27
Ebro	0.19	0.12	0.15	0.22	0.24
Cataluña	**0.22**	0.13	0.16	0.27	0.28
Baleraric	0.15	0.03	0.17	0.24	0.22
Total Domain	0.17	**0.05**	0.15	0.20	**0.24**

Δ DTR (°C/decade)	Annual	DJF	MAM	JJA	SON
North	0.05	0.18	0.11	-0.06	-0.05
Duero	0.12	**0.32**	0.13	0.05	-0.09
Tajo	0.09	0.30	0.10	-0.03	-0.09
Guadiana	0.08	0.26	0.11	-0.02	**-0.10**
Guadaquivir	0.09	0.30	0.15	-0.03	**-0.10**
South	0.16	0.25	0.14	0.11	0.12
Segura	0.19	0.31	0.17	0.14	0.07
Levante	0.08	0.25	0.04	0.02	-0.03
Ebro	0.10	0.25	0.12	0.04	-0.07
Cataluña	0.09	0.16	0.10	0.08	0
Baleraric	0.06	0.10	0.10	0.04	-0.02
Total Domain	0.10	**0.26**	0.12	0.02	**-0.05**

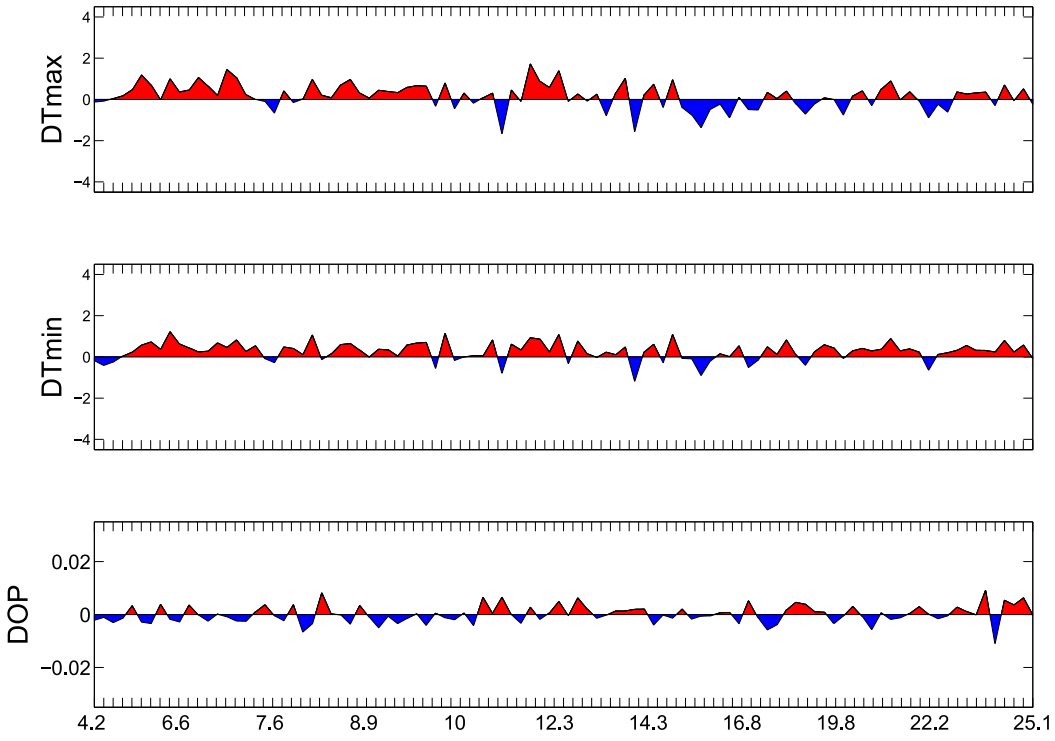

Figure 9: *Top panel*: Differences in maximum temperature (DTmax) for each WT. *Middle panel*: Differences in minimum temperature (DTmin) for each WT. *Bottom panel*: Differences in the occurrence probability of the WTs (DOP). Differences in temperature are calculated in °C.

We can see that the warmest WTs, in terms of mean temperature, increased their frequency of appearance during period 1980-2002, while the coldest WTs decreased it, but, from a global point of view, results are very noisy.

We have done this same analysis seasonally. The results are exposed in figure 10, where upper and middle panels represent the changes of each WT, for maximum and minimum temperatures, respectively, and the bottom panels show the frequency of appearance of each WT. WTs are ordered by their mean temperature in the first period (it is the same order as that of figure 9). The "X", in upper and middle panels, indicates that the WT does not appeared in one or both periods.

Looking at table 4 and figure 10, we can see that during summer and winter not all the WTs were possible, furthermore, WTs that happened during one of these seasons usually did not occur in the other one. Nevertheless, almost all the WTs appeared during autumn and spring, showing the high variability of the atmospheric states for these two seasons over the domain of study.

As it happened in the global case, the most significant changes were more related to changes in the associated temperature of the WTs, than to changes in their probability of appearance, which has shown to be very noisy, as it can be seen in the bottom panel of figure 9

4.4. Example of changes in a Weather Type

Performing a detailed analysis of every WT is beyond the scope of this paper. As a first approach, we have only considered the most general and remarkable conclusions.

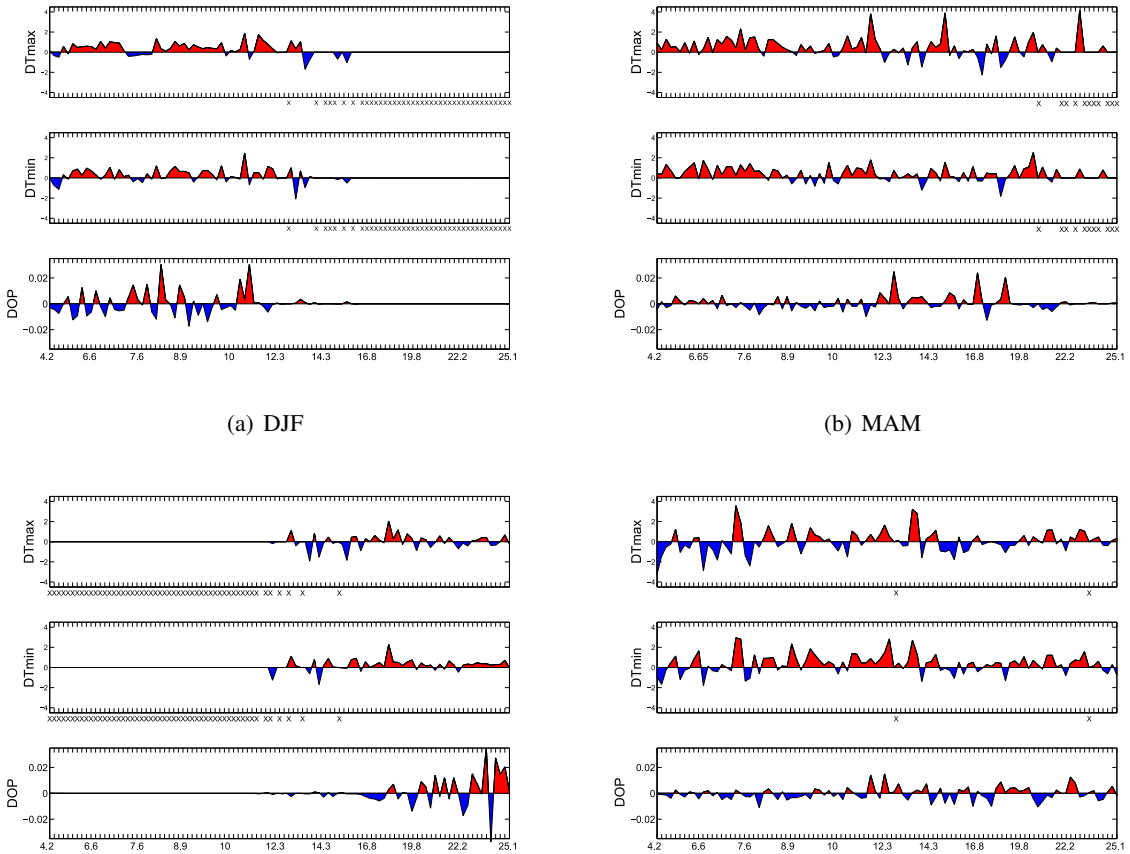

(a) DJF (b) MAM

(c) JJA (d) SON

Figure 10: The same as figure 9 but separated into seasons (°C). "X" indicates that the WT has not appeared during one or both periods.

Table 4: % of WTs, considering those that happened during each season, that increased (⇑), decreased (⇓) or did not change (=) their maximum (**Tx**) and minimum (**Tn**) temperatures and their frequency of appearance (**freq**), annually and seasonally, and also the number of WTs that did not appear during one or both period (**Did not happen**). Increases in temperature are considered to be those changes greater than 0.1 °C, and decreases those changes smaller than -0.1 °C. Those temperature values between these two thresholds are considered as no changes. For the frequency of appearance the selected threshold was ±0.01%, which corresponds to a change of 1 day of appearance every 45 years.

	Annual	**DJF**	**MAM**	**JJA**	**SON**
⇑**Tx**	53	**68.42**	**67.44**	46.67	46.94
=**Tx**	17	5.26	10.47	6.66	7.14
⇓**Tx**	30	26.32	22.09	46.67	45.92
⇑**Tn**	69	56.14	**66.28**	**71.11**	**64.29**
=**Tn**	14	12.28	9.30	8.89	5.10
⇓**Tn**	17	31.58	24.42	20	30.61
⇑**freq**	45	42.11	40.70	35.56	48.98
=**freq**	1	1.75	4.65	2.22	1.02
⇓**freq**	54	56.14	54.65	62.22	50
Did not happen	0	**43**	14	**55**	2

Figure 11 shows an example of a very hot WT: WT54, which is the centroid of the class number 54. We have selected WT54 because it is one of the warmest WTs, for maximum, minimum and mean temperature. It increased its maximum temperature 0.69°C and its minimum temperature 0.79°C. WT54 is one of the WTs that appears, above all, during summer. Besides, WT54 happened 42 times (0.515%) during period 1957-1979 and 87 times (1.051%) during 1980-2002, duplicating its probability of appearance during the second period. Moreover, during 1957-1979, 3 of the 42 days (7.143% of the days) had a mean maximum temperature higher than 35°C, while 11 of the 87 days in period 1980-2002 (12.644% of the days) exceeded that threshold. This figure gives us a general idea of the information that WTs can give us.

As every WT, WT54 is represented by the corresponding surface phenomena (in this example observations of maximum temperatures are shown; figures 11(a), 11(c) and 11(e)) and by the atmospheric circulation pattern, which is represented utilizing the Re-analysis data form ERA-40 (in this example: mean temperature at level 1000hPa (T1000); figures 11(b), 11(d) and 11(f)). The top two figures represent the mean value of maximum temperature and T1000, respectively, for period 1957-1979, while the two figures bellow represent the same as figure 11(a) and 11(b), but for period 1980-2002. Figures 11(e) and 11(f) represent the differences between both periods for maximum temperature observations and T1000, respectively. Except for the resolution, we can see a good agreement between the observations and the ERA-40 Re-analysis data. The bottom figure shows the number of times that the WT appeared during each year, and the red line shows the trend of its frequency of appearance. In this example, the frequency of appearance of the WT rose 107,14% during the second period of study.

We can also see from figure 11(e) that, for WT54, the maximum temperature increased over the Cataluña, the Levante and the South basins, the western side of the Segura basin and the northwest side of the North basin, while in the southwestern side of the peninsula maximum temperature decreased. The conclusions are similar if we focus on figure 11(f). In this graph we can see that mean temperature at 1000hPa increased over the Cataluña basin and the northwest part of the North basin, and it dropped over the southwest of mainland Spain.

5. Discussion and conclusions

We have created homogenized time series, as described in section 3.1, and although they tend to smooth the final results, they show a good agreement with the original series.

We have seen that, comparing period 1957-1979 and period 1980-2002, maximum and minimum temperature increased from 1980 on. The rise in temperature was generalized but not homogeneous over the whole domain, because there were some areas that hardly changed their temperatures, while other areas increased it up to 0.31°C/decade, as it is the case of the Cataluña basin (see table 3). The mean change in maximum temperature, for the whole domain, was an increase of 0.27°C/decade and the mean rise in minimum temperature, for the whole area of study, was 0.17°C/decade.

The northeast of Spain (the Cataluña basin), the center of the peninsula (the eastern side of the Guadiana and Guadalquivir basins) and the oriental side of the Cantabrian watershed (the eastern side of the North basin with the northwest part of the Ebro basin) are the areas with higher differences in extreme temperatures. Thus, these are the regions that suffered a stronger warming in extreme temperatures.

If we study the changes in temperature seasonally, we have to emphasize that maximum temperature increased in a generalized way during winter and minimum temperature hardly changed or slightly decreased during this season. This means that the DTR during this season was higher during period 1980-2002 than during period 1957-1979.

Although maximum temperatures have shown a greater rise than minimum temperatures, WTs show a more generalized increase in minimum temperature. Thus, there are more WTs that increase their minimum temperature than their maximum temperature. Besides, we have also noticed that there is no

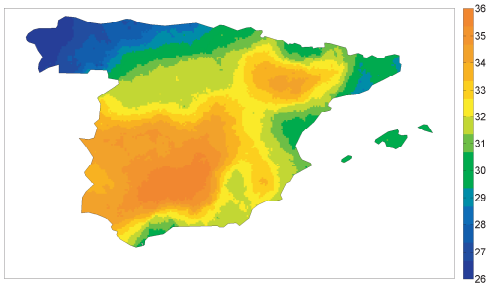

(a) WT54 Observations (1957-1979)

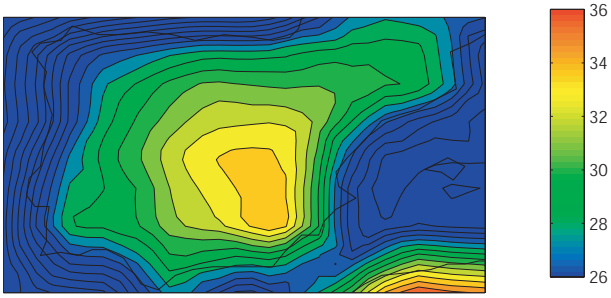

(b) WT54 T1000 from ERA-40 (1957-1979)

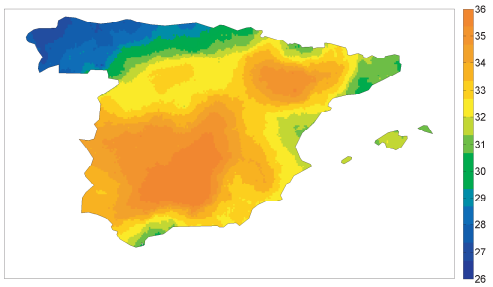

(c) WT54 Observations (1980-2002)

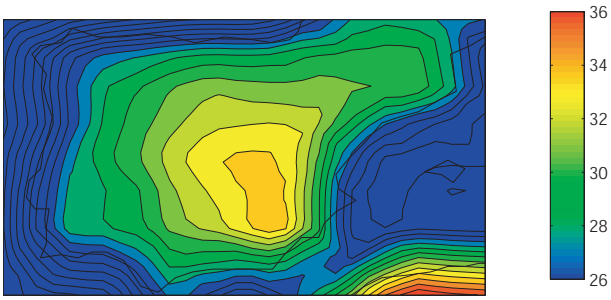

(d) WT54 T1000 from ERA-40 (1980-2002)

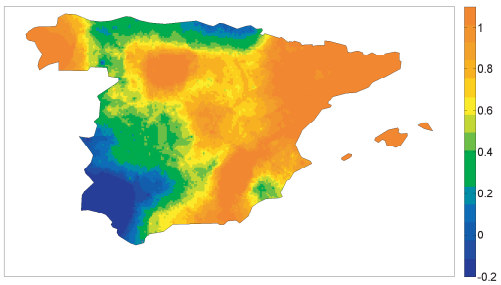

(e) WT54 Difference in observations (11(c) minus 11(a))

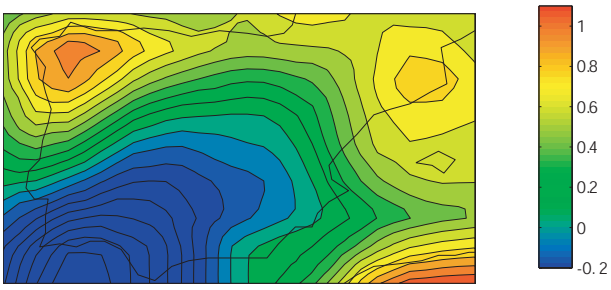

(f) WT54 Difference in T1000 (11(d) minus 11(b))

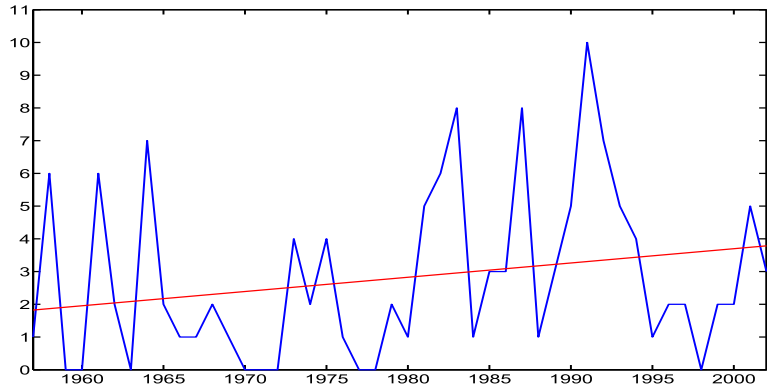

(g) Number of days that WT54 happened each year

Figure 11: WT54 for maximum temperature observations data (figures 11(a), 11(c) and 11(e)) and mean temperature at level 1000hPa (T1000) from ERA-40 Re-analysis data (figures 11(b), 11(d) and 11(f)). Figures 11(a) and 11(b) represent maximum temperature and T1000 for period 1957-1979, respectively, while figures 11(c) and 11(d) represent the same for period 1980-2002. Figures 11(e) and 11(f) represent the differences between both periods for maximum temperature and T1000, respectively. Figure 11(g) shows the number of days that this WT appears each year (blue line) and the trend of its frequency of appearance, also expressed in number of days (red line).

significant change in their occurrence probability. Nevertheless, from figure 9, two of the three warmest WTs were more frequent during the second period of study (1980-2002), while the three coolest ones decreased their occurrence probability.

In conclusion, changes in the extreme temperatures were heterogeneous in space, as we have seen in figure 6, in time, as it is shown in the seasonal decomposition (table 3 and figures 7 and 8) and in the distribution of WTs, as shown by figures 9 and 10.

All the local observed trends are in good agreement with those described globally in IPCC (2007), with one remarkable exception: possitive trends in DTR during winter.

Acknowledgements

This work has been possible thanks to the AEMET's post-graduate training program (2009); project No. 7: *"Adaptation of statistical downscaling methods to climatic timescales over the Cantabrian coast"*.

References

Action COST 733 (2005): Harmonisation and Application of Weather types classifications for European Regions. *Proceedings from 5th annual meeting of the Eurpean Meteorological Society*, Session AW8. URL www.cost.esf.org/library/publications/07-49-Session-AW8-Weather-Types-Classifications.

Alexandersson H (1986): A homogeneity test applied to precipitation data. *J. Climatol.*, 6:661–675.

Ancell R and Gutiérrez JM (2008): High resolution probabilistic forecast using Bayesian networks. *EMS Annual Meeting 2008. European Conference on Applied Climatology (ECAC)*.

Anderberg MR (1973): *Cluster Analysis for Applications*. Press, New York.

Bárdossy A and Caspary HJ (1990): Detection of climate change in Europe by analysing European atmospheric circulation patterns from 1881 to 1989. *Theor. Appl. Climatol.*, 42:155–167.

Brunet M, Jones PD, Sigró J, Saladié O, Aguilar E, Moberg A, Della-Marta PM, Lister D, Walther A and López D (2007): Temporal and spatial temperature variability and change over Spain during 1850-2005. *J. Geophys. Res.*, 112:D12117. doi:10.1029/2006JD008249.

Cano R and Gutiérrez JM (2004): Relleno de lagunas y homogeneización de series de precipitación en redes densas a escala diaria. *El clima, entre el Mar y la Montaña*, Serie A, nº 4. URL www.aeclim.org/publiac.html.

Conrad V and Pollack LD (1962): *Methods in Climatology*, volume 4.2. Harvard University Press.

Diaz HF (1981): Eigenvector analysis of seasonal temperature, precipitation and synoptical-scale frecuency over the contiguous United States. Part II: Spring, summer, fall and annual. *Mon. Weather Rev.*, 109:1285–1304.

Esteban P, Martin-Vide J and Mases M (2006): Daily atmospheric circulation catalogue for western europe using multivariate techniques. *Int. J. Climatol.*, 26:1501–1515.

Gutiérrez JM, Cano R, Cofiño AS and Rodríguez MA (2004a): Clustering Methods for Statistical downscaling in Short-Range Weather Forecast. *Monthly Weather Review*, 132(9):2169–2183.

Gutiérrez JM, Cano R, Cofiño AS and Sordo CM (2004b): *Redes Probabilísticas y Neuronales en las Ciencias Atmosféricas*. Series Monográficas de AEMET.

Hewitson BC and Crane RG (2002): Self-organizing maps: applications to synoptic climatology. *Climate Res.*, 22:13–26.

Huth R, Nemesová I and Klimperová N (1993): Wheather categorization based on the average linkage clustering technique: an application to European mid-latitudes. *Int. J. Climatol.*, 13:817–835.

IPCC (2007): Fourth Assessment Report (IPCC AR4). *Geneva: Intergovernmental Panel on Climate Change*.

Jones PD and Lister DH (2009): The influence of the circulation on surface temperature and precipitation patterns over Europe. *Clim. Past*, 5:259–267.

Kohonen T (1997): Exploration of very large databases by self-organizing maps. *IEEE International Conference on Neural Networks (ICNN 97)*.

Lamb HH (1972): British Isles weather types and a register of daily sequence of circulation patterns, 1861-1971. *Geophys. Mem.*, 15:116–185.

Lamb HH (1977): *Climate, present, past and future. Climatic History and the Future*, volume 2. London Methunen & Co.

Lorenz EN (1969): Atmospheric predictability as revealed by naturally occuring analogues. *J. Atmos. Sci.*, 26:636–646.

Pastor MA, Casado MJ and Doblas-Reyes FJ (2008): Climate model validation in the Euro-Atlantic domain using circulation types. *Area de Evaluación y Modelización del Cambio Climático de AEMET*, Nota Técnica 4. (NT AEMCC-4).

Philipp A, Della-Marta PM, Jacobeit J, Fereday DR, Jones PD, Moberg A and Wanner H (2007): North Atlantic-European pressure patterns since 1850 classified by semulated annealing clistering. *J. Climate*, 20:4065–4095.

Preisendorfer RW and Mobley CD (1988): *Principal component analysis in meteorology and oceanography*. Elsevier, Amsterdam.

Sneyers R (1975): Sur l'analyse statistique des séries d'observations. *WMO Tech. Note*.

Uppala SM, Kållberg PW, Simmons AJ, Andrae U, da Costa Bechtold V, Fiorino M, Gibson JK, Haseler J, Hernández A, Kelly GA, Li X, Onogi K, Saarinen S, Sokka N, Allan RP, Andersson E, Arpe K, Balmaseda MA, Beljaars ACM, van de Berg L, Bidlot J, Bormann N, Caires S, Chevallier F, Dethof A, Dragosavac M, Fisher M, Fuentes M, Hagemann S, Hólm E, Hoskins BJ, Isaksen L, Janssen PAEM, Jenne R, McNally AP, Mahfouf JF, Morcrette JJ, Rayner NA, Saunders RW, Simon P, Sterl A, Trenberth KE, Untch A, Vasiljevic D, Viterbo P and Woollen J (2005): The ERA-40 re-analysis. *Q. J. Roy. Meter. Soc.*, 131:2961–3012. doi:10.1256/qj.04.176.